


# Outlook of Covid-19 Curing through Structural and Electronic Properties of Natural Drugs

Sara Shahriari <sup>1</sup>, Karim Zare <sup>2</sup>, Fatemeh Mollaamin <sup>3,\*</sup> 

<sup>1</sup> Department of Chemistry, Central Tehran Branch, Islamic Azad University, Tehran, Iran

<sup>2</sup> Department of Chemistry, Science and Research Branch, Islamic Azad University, Tehran, Iran

<sup>3</sup> Department of Biomedical Engineering, Faculty of Engineering and Architecture, Kastamonu University, Kastamonu, Turkey

\* Correspondence: [smollaamin@gmail.com](mailto:smollaamin@gmail.com) (F.M.);

Scopus Author ID 35848813100

Received: 27.03.2022; Accepted: 29.04.2022; Published: 11.09.2022

**Abstract:** Humans and multiple species of animals must be infected by coronaviruses (positive-stranded RNA viruses) through enteric, respiratory, and central nervous system sickness with attractive targets for designing anti- Covid-19 conjunction. In this work, it has been investigated the compounds of luteolin-7- glucoside, curcumin, epicatechin-gallate, allicin, and zingerol as probable anti-pandemic Covid-19 receptors derived from medicinal plants. Anti-Covid-19 through the hydrogen bonding using the physicochemical features consisting of thermodynamic parameters, nuclear magnetic resonance analysis, and IR characteristics, of luteolin-7- glucoside, curcumin, epicatechin-gallate, allicin, and zingerol compounds binded to the fragment of Tyrosine-Methionine-Histidine as the selective area of the Covid-19, IR frequency and intensity of various normal modes of these structures have been estimated. The theoretical calculations were accomplished at different steps of theory to achieve the more accurate equilibrium geometrical consequences, and IR spectral analysis for each of the complex drugs of O-terminal or N-terminal auto-cleavage substrate were approved to clear the structural flexibility and substrate attaching of seven medicinal plants bonded to the active site of Covid-19 molecule. Comparing these compounds with two configurations prepares a new outlook for the design of substrate-based anti-targeting of Covid-19. This indicates a feasible model for designing a wide spectrum of anti-Covid-19 drugs. The compounds-based energy minimization of these materials has resulted in two more effectual lead compounds, N and O atoms, forming the hydrogen bonding (H-bonding) with potent anti- Covid-19. Finally, two medicinal ingredients of allicin, curcumin, luteolin-7- glucoside, and zingerol bonded to TMH have been directed to a Monte Carlo (MC) simulation and UV-Visible for estimating the absorbance of luteolin-7- glucoside, and epicatechin-gallate.

**Keywords:** luteolin-7- glucoside; curcumin; epicatechin-gallate; allicin; zingerol; Covid-19; NMR; IR; UV-Visible.

© 2022 by the authors. This article is an open-access article distributed under the terms and conditions of the Creative Commons Attribution (CC BY) license (<https://creativecommons.org/licenses/by/4.0/>).

## 1. Introduction

The epidemiological situation in South Africa has been identified by three different peaks in announced cases, the latest of which was predominantly the Delta variant. Then, infections increased sharply, simultaneously with finding B.1.1.529 variant. The SARS-CoV-2 variant: B.1.1.529 was monitored and evaluated by experts of the technical advisory group on SARS-CoV-2 Virus Evolution in 2021.

This variant has a grand number of mutations, some of which are worrying. This variant has an increased risk of reinfection compared to other VOCs. So, current SARS-CoV-2 PCR

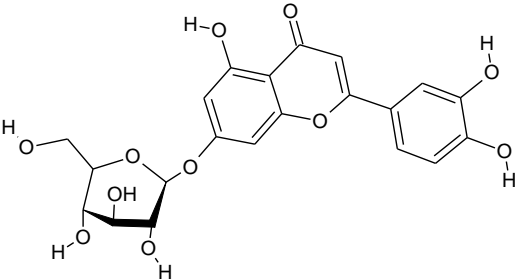
diagnostics can find this variant. Some experiments have shown that for one large PCR test, one of the three target genes is not found, and this test can be applied as a sign for this variant, waiting for sequencing approval. By this method, this variant has been found at more rapid amounts than previous waves in infection, recommending that this variant might have a growth privilege. It has been approved that a detrimental change in Covid-19 epidemiology should be determined as a VOC, and the WHO has determined Covid-19.

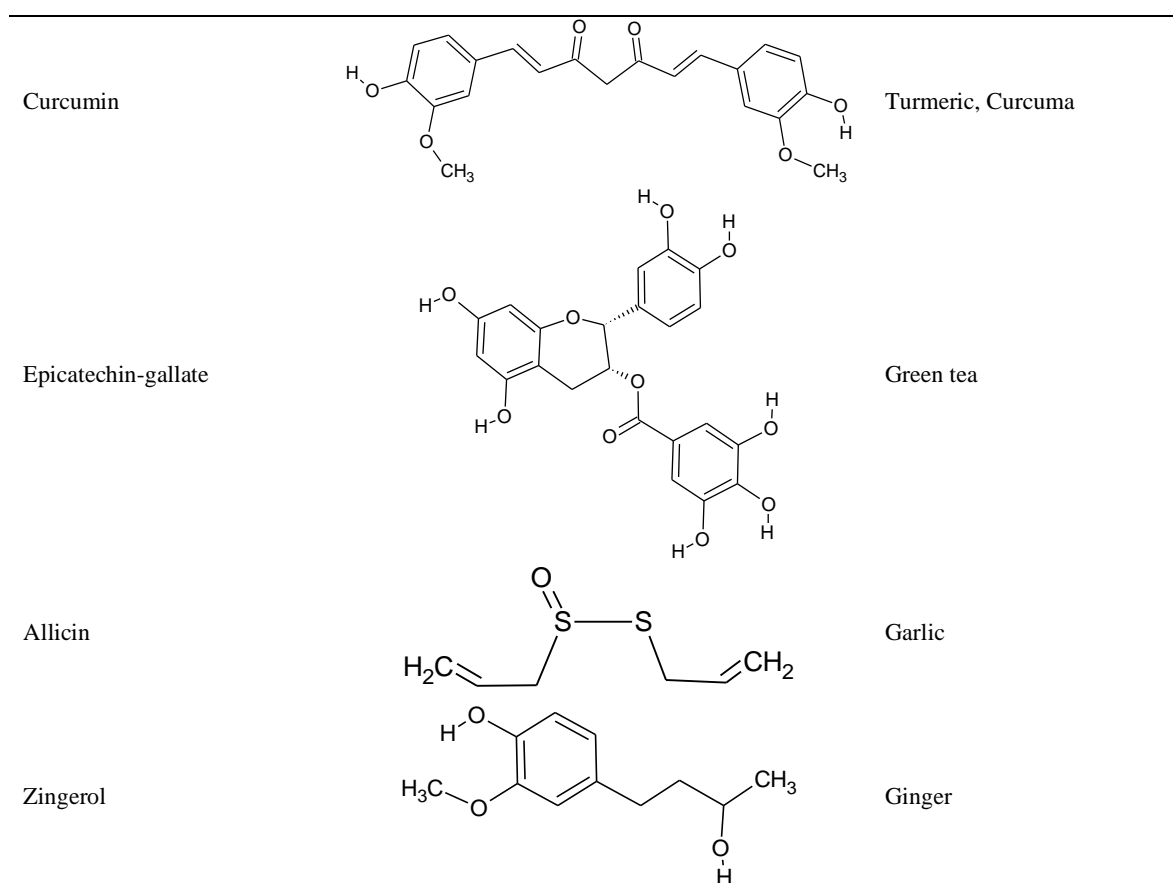
People are reminded to take measures to decrease their risk of Covid-19, consisting of public health and social measures such as wearing masks, hand hygiene, physical distancing, increasing ventilation of inside spaces, preventing crowded spaces, and getting vaccinated [1-3]. It has been announced that the global outbreak of special life-threatening pneumonia resulted in about 800 deaths which were world identified as the harsh syndrome CoV (SARS-CoV) [4-8]. In addition, improved research has exhibited that the source of SARS-CoV based on the phylogenic discussion is most likely from bats converted to human aerosols because of intermediate hosts such as infectious palm civets by the virus [9-11]. CoV closely relates to strong breathing syndrome CoV (SARS-CoV), which is an epidemic with a short period of living time.

Moreover, MERS-CoV indicates SARS-like symptoms through human infections, consisting of the signs like influenza: high fevers, fatigue, malaise, and rigors, but it has been observed later improvement into typical pneumonia in most samples. Therefore, the animal patience of CoV, through its power of intermediate transition into the human, is threatening that has been concluded with a new case of MERS-CoV recommending bats and dromedary camels as the source for this kind of virus sample [12-18].

In some works, it has been explored that a prototype of the Coronaviridae family is an infectious bronchitis virus (IBV) which corresponds to the genetic group III of CoV and produces a serious economic problem for the poultry sources in the world society [19-22]. In fact, the researchers have not achieved any vaccine or specific antiviral cures by managing the treatment of symptoms and collecting experimental information [23-25]. Environmental elements can greatly affect the secretion of secondary metabolites from tropical plants. Therefore, great attention has been paid to the secondary metabolites conducted by plants in tropical regions that may be developed as medicines [26-28]. Several compounds, such as flavonoids, from medicinal plants, have been reported to have antiviral bioactivities [29-31]. In the present study, we investigated luteolin-7- glucoside, curcumin, epicatechin-gallate, allicin, and zingerol as the probable anti- Covid-19 receptor derived from medicinal plants (Table 1).

**Table 1.** Medicinal ingredients of luteolin-7- glucoside, curcumin, epicatechin-gallate, allicin, and zingerol as the probable anti-Covid-19 receptor derived from medicinal plants.

Compound	Molecular structure	Sources
Luteolin-7- glucoside		Olive, Star fruit, Chili pepper, Welsh onion/ Leek



The findings of the present study will provide other researchers with opportunities to identify the right drug to combat Covid-19 by theoretical methodologies to guess the effect of hydrogen bonding in various attachment through seven medicinal plants of Luteolin-7-glucoside, curcumin, epicatechin-gallate, allicin and zingerol bonded to the active site of Covid-19 PDB.

## 2. Material and Method

The linkage of luteolin-7- glucoside, curcumin, epicatechin-gallate, allicin, and zingerol bonded to the active site of Covid-19 protein has been accomplished in this work by forming relatively stable complexes through hydrogen bonding. Therefore, one series of quantum force fields, including m062x/cc-pvdz pseudo=CEP for complexes of seven inhibitors for Covid-19, has been accomplished through discovering the minimized coordination of the best molecules of natural plant-TMH drug design sample with IR calculations using the Gaussian09 software [32]. It has been remarked that polarization functions into the employed basis set in the theory always presents a magnificent achievement in the simulation and modeling of theoretical studies. Then, normal mode results are discovering potential harmonic wells by analytic methodologies that save the movement of all atoms simultaneously in the vibration time range toward a natural discussion of structural vibrations [33-38]. So, the minimized geometry coordination of medicinal ingredients-TMH complexes toward the drug design has been run through the active site of certain O, N, and H atoms in the linkage of bond and torsion angles (Table 2).

**Table 2.** The optimized characteristics of Luteolin-7- glucoside, curcumin, allicin, and zingerol bonded to TMH active site through the drug design method.

Medicinal structures – Covid-19 target	Bond length	(Å)	Bond/Torsion angle	(°)
<b>Luteolin-7- glucoside</b>	N100-H101	1.0098	N100- H101-O32	155.138
	H101-O32	0.9362		
	O32-C13	1.3606	N100-H101-O32-C13	-88.906
<b>Curcumin</b>	N95-H96	1.0099	N95-H96-O9	117.254
	H96-O9	0.9706		
	O9-C6	1.3621	N95-H96-O9-C6	78.7092
<b>Allicin</b>	C37-O38	1.3600	C37-O38-H39	112.999
	O38-H39	0.9600		
	H39-S4	1.5042	C37-O38- H39- S4	41.807
<b>Zingerol</b>	N78-H79	1.0100	N78-H79-O11	130.223
	H79-O11	0.9966		
	O11-C9	1.4087	N78-H79-O11-C9	148.048

So, for achieving a constant molecule of medicinal plant linkage of the Covid-19 active site, geometry optimization plus the nuclear magnetic resonance estimation, intensity, and harmonic frequency of different normal modes were computed with ab initio methods, and the IR spectra were analyzed [39, 40]. The theoretical computations were run at different levels of calculations to achieve more accurate equilibrium geometrical consequences and infrared spectral information for each of the certain molecules. It is recommended that polarization functions and an additional diffuse into employed basis sets in the calculation significantly improve the consequences of theoretical levels. The simulation exhibits the methodologies that produce a common model template at a particular temperature by measuring all physicochemical characteristics through the partition functions [34].

Each part of the model consisting of natural components-TMH has been minimized by quantum mechanic calculation of DFT level, including ECP computations with pseudo=CEP basis sets. Moreover, these systems have been estimated by QM/MM method due to the ONIOM method.

In our research, force field differences are debated by comparison of energies and density with AMBER and OPLS force fields via MC minimization. Besides, a Hyperchem professional release 7.01 program has been employed for additional keywords like PM3MM, PM6, and pseudo=CEP [41, 42].

Moreover, Monte Carlo simulation (MC) has been accomplished on the anti-Covid-19 drugs. This approach is a group of theoretical algorithms based on repeated random cases to evaluate the consequences, usually employed in the simulation of mathematical and physical models.

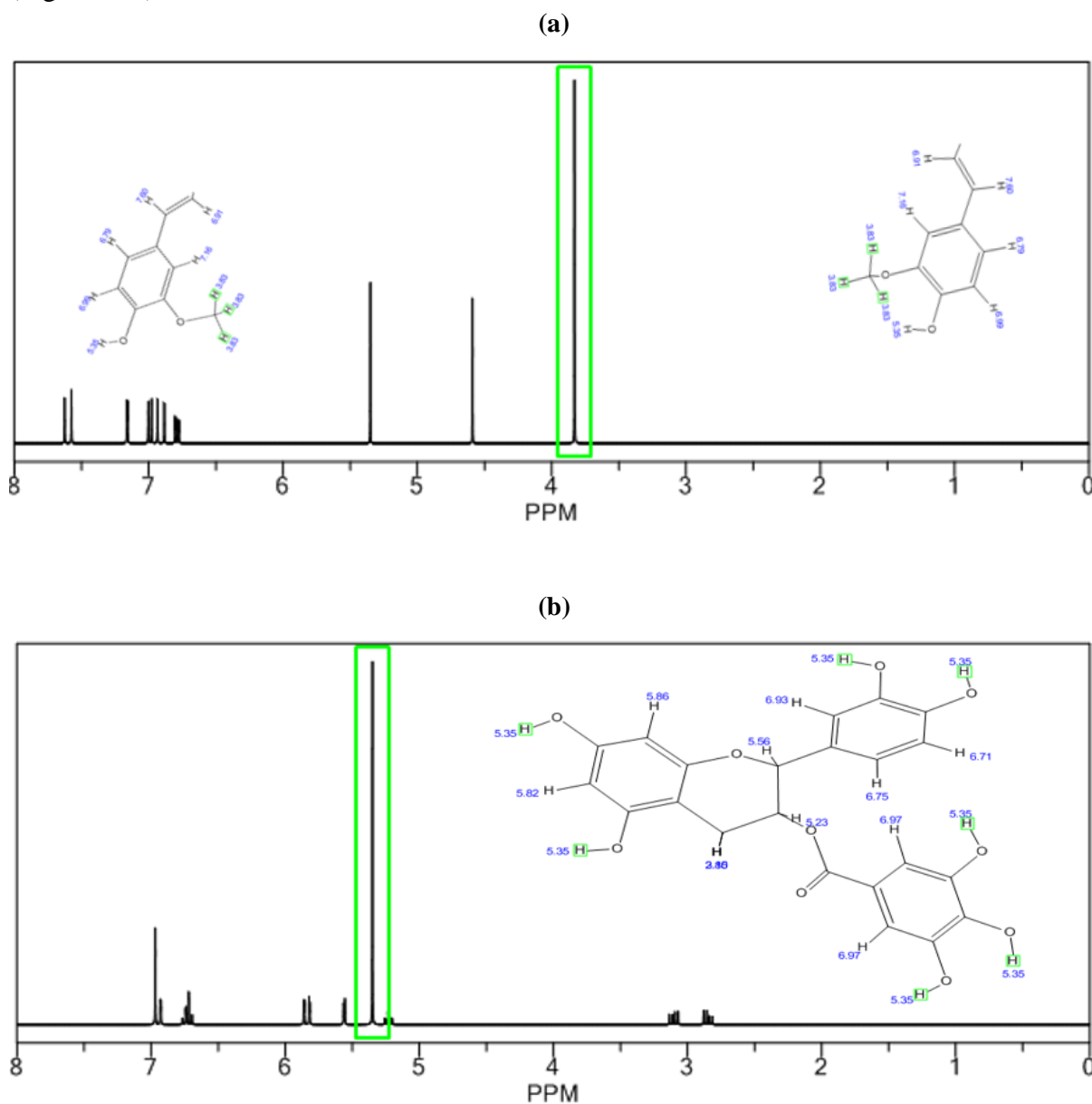
Calculation of pseudo-random or random amounts generates computation accuracy, particularly for the impossible or unfeasible calculation to a precise consequence with a deterministic algorithm amount [43]. Applying deterministic, pseudo-random sequences doesn't need random numbers, causing it easy to examine and redo the simulation levels [44]. A novel configuration is approved if the energy reduces and with a possibility of  $e^{-\Delta E/kT}$  if the energy enhances. This Metropolis process ensures that the configurations in the ensemble follow a Boltzmann distribution, and the probability of proving higher energy configurations permits Monte Carlo force fields to go up and flee from a local minimum well [44].

Monte Carlo force fields need only the capability to estimate the system's energy, which might benefit if computing the first derivative is hard or time-consuming. Moreover, since only a single particle is passed in each step, only the energy altering accompanied by this motion

should be computed, not the total energy for the total system. A benefit of Monte Carlo methods is the loss of time dimension and atomic speeds, so they are not appropriate for investigating features relating to momentum or time-dependent phenomena [44].

### 3. Results and Discussion

The computation of hydrogen nuclear magnetic resonance  $^1\text{H}$ -NMR on the foundation of amino acids in the beta-sheet conformation Tyrosine-Methionine-Histidine and the four main ingredients of medicinal plants, including curcumin, epicatechin-gallate, allicin, and zingerol oleuropein, and quercetin have been evaluated to explore the certain atoms of hydrogen, nitrogen, and oxygen in the critical areas of these anti-virus medicines through the generating of H-bonding by identifying the attack point of Tyrosine-Methionine-Histidine (Figure1a-d).



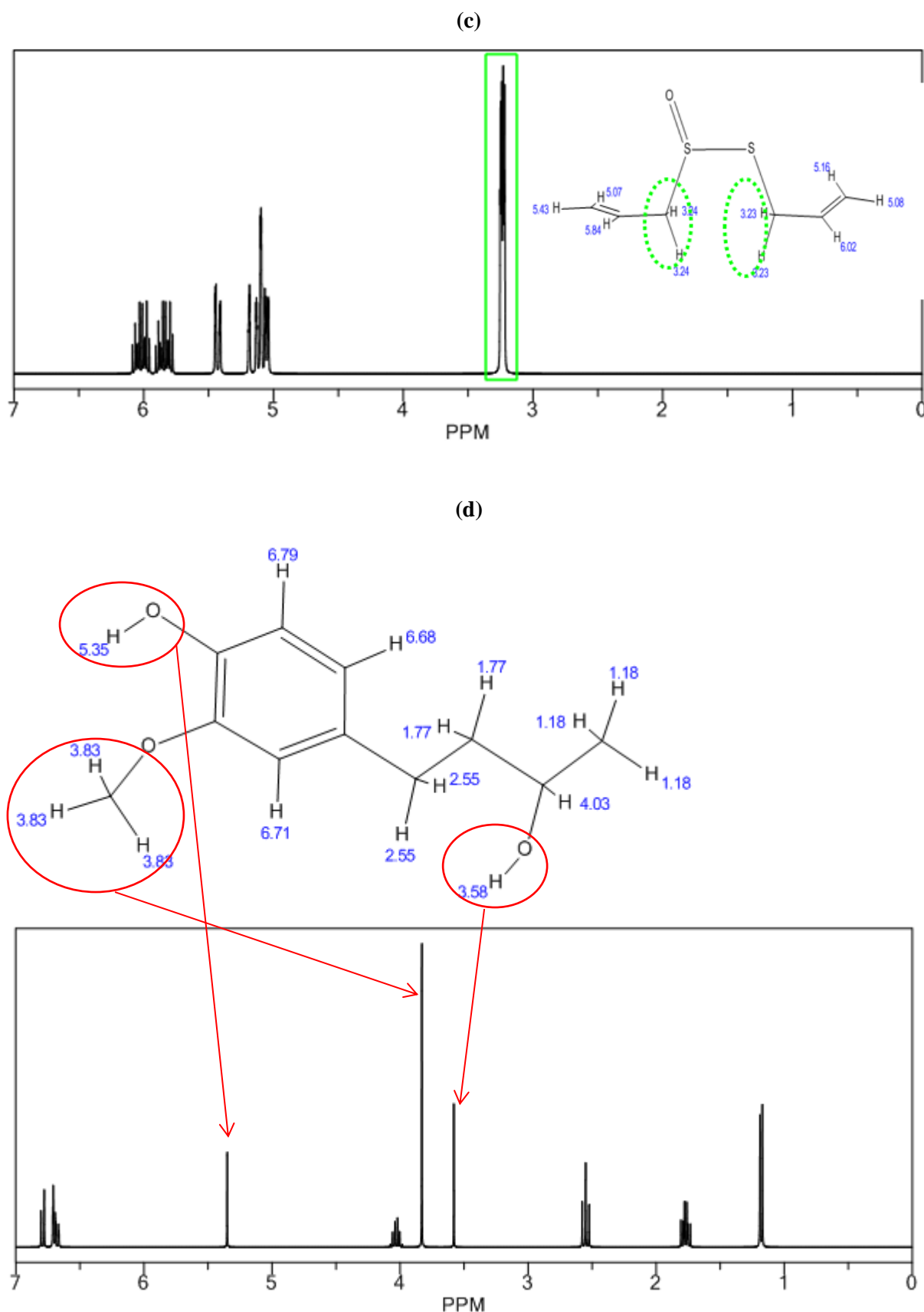


**Figure 1.** NMR spectra of (a) curcumin; (b) epicatechin-gallate; (c) allicin; (d) zingerol bonded to TMH Covid-19 active site through the drug design method by showing the active region of TMH in the drug design process.

The nuclear magnetic resonance analysis shows the critical points of the principal components of medicinal plants for binding to the Tyr160-Met161-His162 (TMH) due to producing the anti-virus drugs. In contrast, each active atom of O and N as the electronegative

atoms for binding to the H remarks the maximal shift in all steps in the NMR spectrum [45-52] (Figure 1 a-d).

Then two main ingredients of medicinal plants, including allicin and curcumin, were computed for strengthening the linkage of Tyr160-Met161-His162 as the anti-Covid-19 drug using the drug design model by infrared spectroscopy at Gaussian09 program software (Figure 2 a,b).

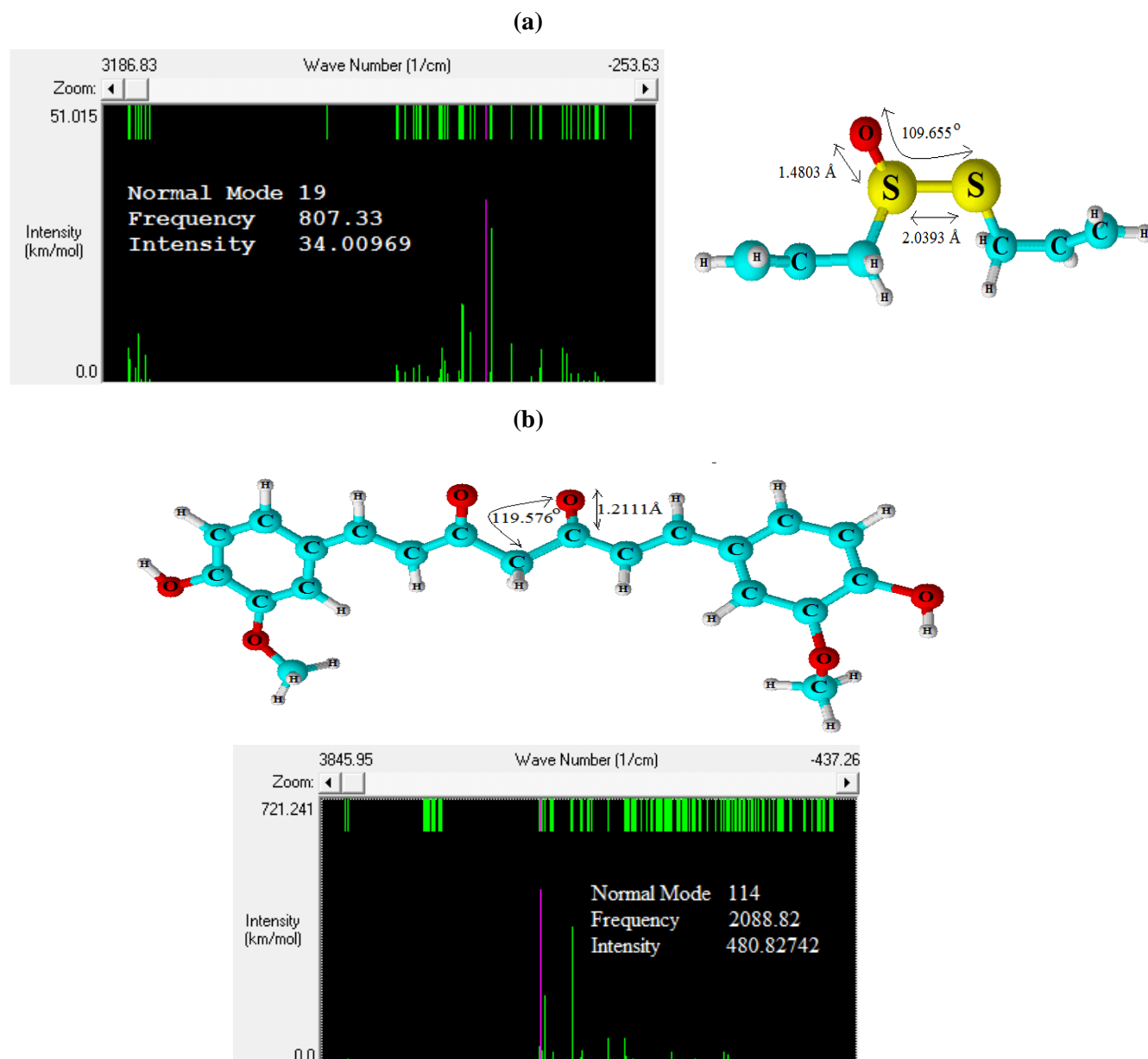


**Figure 2.** IR spectrum of (a) allicin and (b) curcumin bonded to TMH through the drug design method calculated by m062x/cc-pvdz pseudo=CEP.

Moreover, the difference of  $\Delta H_F$  among Luteolin-7- glucoside, curcumin, allicin, and zingerol bonded to Covid-19 has been discussed in the H-bonding due to the basis of amino acids in the beta-sheet feature; Tyr160-Met161-His162 as the critical point of the Covid-19 protein (Table 3, Figure 3).



**Table 3.** The heat of formation,  $\Delta H_F$  (kcal/mol), among luteolin-7- glucoside, curcumin, allicin, and zingerol bonded to Covid-19 active site (TMH) complexes at 300 K.

$\Delta H_{\text{Luteolin-7- glucoside}}$	$\Delta H_{\text{(Luteolin-7- glucoside -active site)}}$	$\Delta H_F \times 10^{-4} = \Delta H_{\text{(Luteolin-7- glucoside - active site)}} - (\Delta H_{\text{Luteolin-7- glucoside}} + \Delta H_{\text{active site}})$
-290.8969	997295.3023	99.7560
$\Delta H_{\text{Curcumin}}$	$\Delta H_{\text{(Curcumin - active site)}}$	$\Delta H_F \times 10^{-4} = \Delta H_{\text{(Curcumin - active site)}} - (\Delta H_{\text{Curcumin}} + \Delta H_{\text{active site}})$
-80.7086	-60.3582	-25.8221
$\Delta H_{\text{Allicin}}$	$\Delta H_{\text{(Allicin - active site)}}$	$\Delta H_F \times 10^{-4} = \Delta H_{\text{(Allicin - active site)}} - (\Delta H_{\text{Allicin}} + \Delta H_{\text{active site}})$
28.3617	301334.2727	30.1280
$\Delta H_{\text{Zingerol}}$	$\Delta H_{\text{(Zingerol -TMH)}}$	$\Delta H_F \times 10^{-4} = \Delta H_{\text{(Zingerol -TMH)}} - (\Delta H_{\text{Zingerol}} + \Delta H_{\text{TMH}})$
-101.8283	491670.2132	49.1746

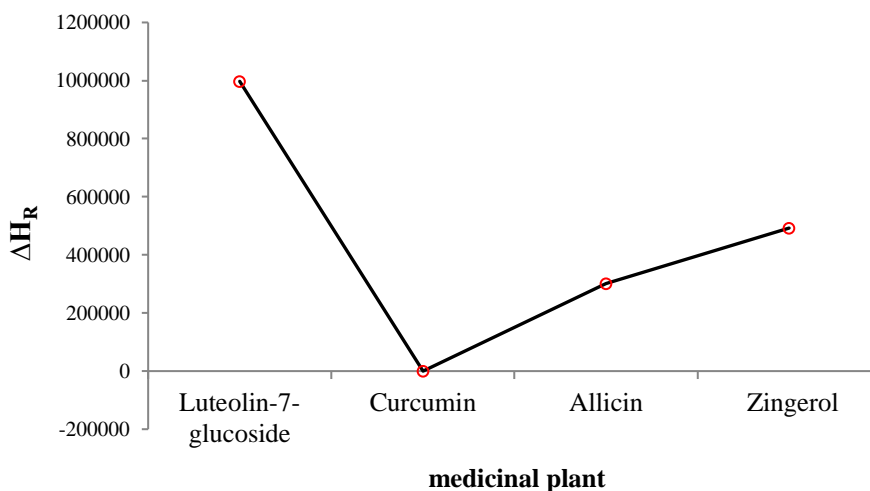


**Figure 3.** The difference of  $\Delta H_F$  among Luteolin-7- glucoside, curcumin, allicin, and zingerol bonded to Covid-19 active site (TMH) complexes at 300 K.

For the next level, the atomic charge of exhibited atoms of O- junction of luteolin-7- glucoside, curcumin, epicatechin-gallate, and zingerol with Tyrosine-Methionine-Histidine have been measured in the region of H-bonding existence (Table 4).

**Table 4.** The values of atomic charge for labeled oxygen atoms in the attachment of luteolin-7- glucoside, curcumin, epicatechin-gallate, and zingerol with Tyr160-Met161-His162.

Luteolin-7- glucoside	charge	curcumin	charge	Epicatechin- gallate	charge	Zingerol	charge
O10	-0.0964	O9	-0.2143	O9	-0.1837	O11	-0.3202
O24	-0.3160	O18	-0.3137	O12	-0.2407	O12	-0.2373
O25	-0.3041	O19	-0.3139	O19	-0.3960	O13	-0.2051
O26	-0.3403	O25	-0.2046	O26	-0.2326		
O28	-0.3417	O26	-0.2046	O27	-0.2524		
O29	-0.1883	O26	-0.2318	O28	-0.2273		
O30	-0.3368			O29	-0.2258		
O31	-0.2135			O30	-0.2114		
O32	-0.2090			O31	-0.2115		
				O32	-0.2491		

Then, in Figure 4, it has been plotted the changes in atomic charge for labeled oxygen atoms through optimized luteolin-7- glucoside, curcumin, epicatechin-gallate, and zingerol with Tyr160-Met161-His162 complexes due to the production of H-bonding. Therefore, the consequences of table 4 in a polar region have represented the strength of Covid-19 medicine, which has been simulated using the drug design model [53-62].

The biggest critical point in Figure 4 has been observed for the samples of epicatechin-gallate, luteolin-7- glucoside, zingerol, and curcumin, respectively, with Tyr160-Met161-His162 considering the oxygen as the electronegative atoms in the formation the H-bonding due to usage of the drug design model which has recommended the simulation of anti- Covid-19.



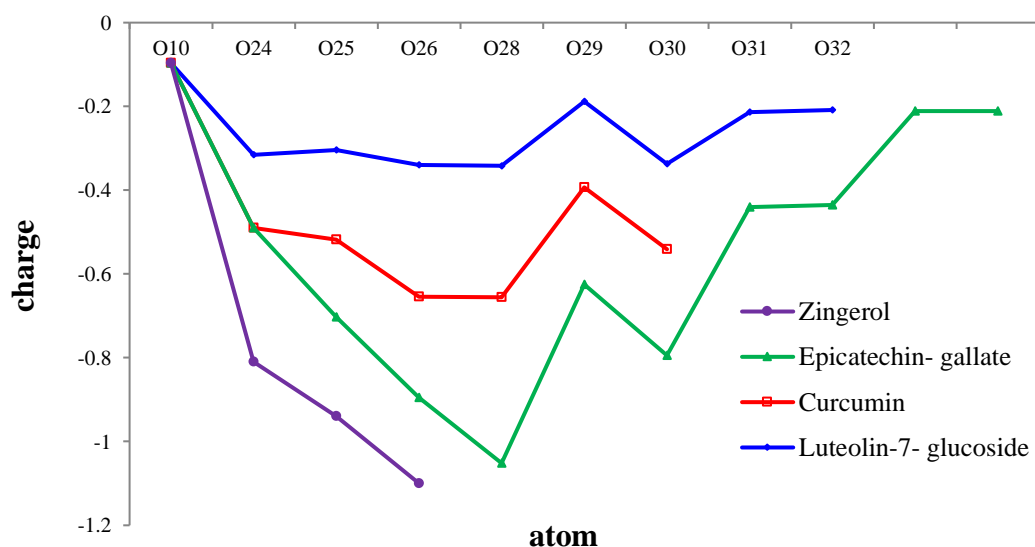


**Figure 4.** Comparing the atomic charge via certain O atoms binding to active sites of luteolin-7- glucoside, curcumin, epicatechin-gallate, and zingerol with Tyr160-Met161-His162.

Therefore, the outlook of Figure4 has suggested the key for the consequences of electronic charge of atoms on medicinal plant- Covid-19 complexes as the anti- Covid-19 drugs, which are basically corresponded to the cite of critical points of certain O, N, and H atoms in the attachment of bond angles. So, the partial charges and spin density have been achieved by matching the electrostatic potential to make constant the charge of O and N with high electronegativity in the linkage of the electrophilic components of H in the foundations of drug plant- Covid-19 as the anti-virus medicines which lead us toward the industry of drug design model [63-69].

Then, allicin, curcumin, Luteolin-7- glucoside, and zingerol bonded to TMH have directed to an MC force field of simulation by potential energy in temperature of 300K versus time range (0-100) due to maximum delta and time steps the amount of 0.05 Å and 1 Å, respectively (Figure 5). So, optimal amounts are near about 0.5. Changing the step size value might greatly impact the considerable ratio. The options dialog box of the Monte Carlo force field conducts us to manage the MC simulation features with 100 steps [70-74].

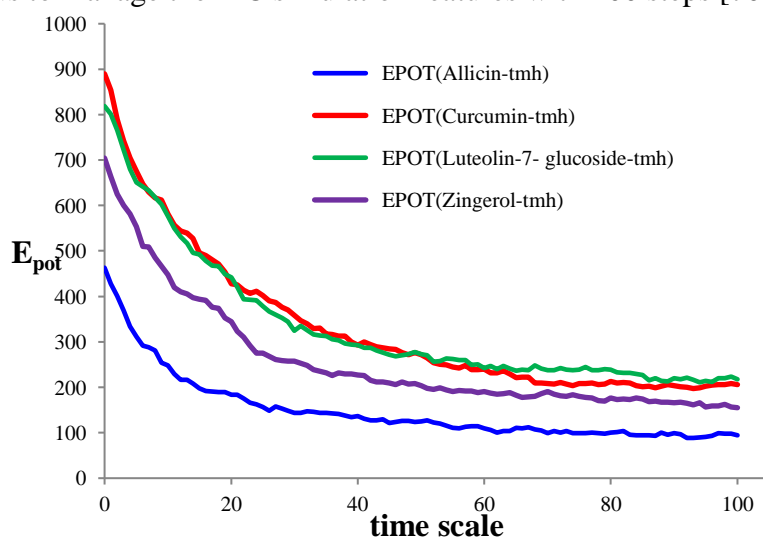


**Figure 5.** Monte Carlo simulation of allicin, curcumin, luteolin-7- glucoside, and zingerol bonded to TMH as the anti-Covid-19 drugs.

The study of the solute-solvent model has encouraged much consideration among scientists, and much research has been accomplished in this area [75-77]. H<sub>2</sub>O characteristic such as dipole moment and dielectric constant makes it a fundamental condition in most biological reactions. It has been evaluated the capability of allicin, curcumin, Luteolin-7-glucoside, and zingerol by HyperChem 8 program software [45]. It has been indicated the PE surface of energy for allicin, curcumin, Luteolin-7- glucoside, and zingerol in the periodic box of H<sub>2</sub>O molecules simulation due to about 0 to100 time scale at 300 K by Monte Carlo force field. The consequences of those experiments lead us to various information surrounding allicin, curcumin, Luteolin-7- glucoside, and zingerol in the model of solute-solvent using appropriate wave function and basis sets induced due to changes in polarity of the medium. Notably, increasing the dielectric constants enhances the power of these anti-Covid-19 drugs [78-82]. Ultraviolet-visible spectroscopy has characterized the compounds that absorb UV radiation passing through the reaction cell and alter the absorbance due to the reaction mechanism. This technic can be applied in the analysis of pharmaceuticals because many drugs are either in the state of unrefined material or in the state of the formulation. They can be evaluated by making a proper drug solution in a solvent and estimating the absorbance at a specific wavelength.

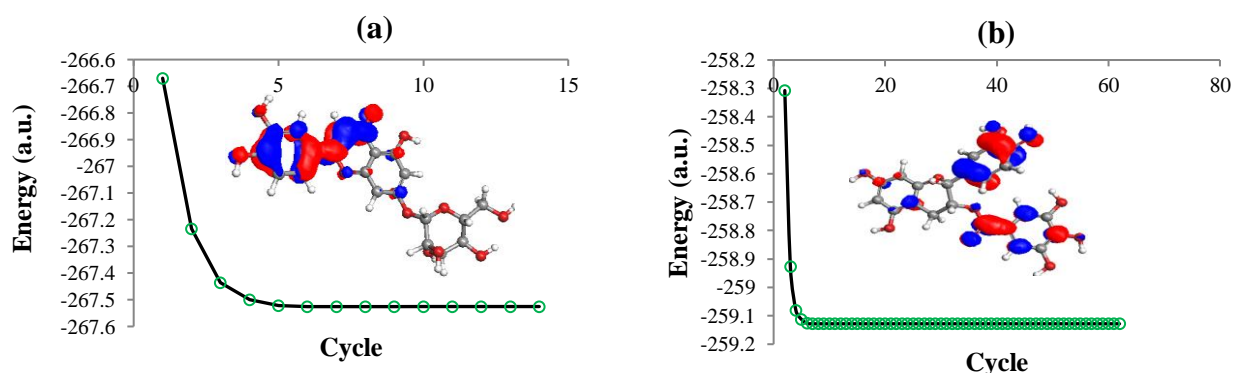


**Figure 6.** The energy changing of the ultraviolet and visible spectrum for absorption of medicinal plants of (a) luteolin-7- glucoside and (b) epicatechin-gallate.

In this investigation, UV-Vis absorption spectra of medicinal plants of luteolin-7-glucoside and epicatechin-gallate have been accomplished due to the possibility of treatment for Covind19 medication (Figure 6).

#### 4. Conclusions

Natural medications of luteolin-7- glucoside, curcumin, epicatechin-gallate, allicin, and zingerol are capable of joining the basis of amino acids components of Tyrosine-Methionine-Histidine as the target area of the Covid-19 by exhibiting the changes in their intensity and harmonic frequency spectra after evaluation using nuclear magnetic resonance methodology which is influenced by the atomic configuration of the anti-virus medicines.

The power of hydrogen bonding between several medicinal ingredients of Luteolin-7-glucoside, curcumin, epicatechin-gallate, allicin, and zingerol and Covid-19 through the formation of anti- Covid-19 with two probabilities of N $\cdots$ H and O $\cdots$ H linkage considering different atomic charges have been investigated using IR methods. So, the thermodynamic properties of Gibbs free energy, enthalpy of formation, Electronic Energy, and Core-Core

interaction have approved the stability of anti- Covid-19 due to H-bonding formation using the drug design method.

The simulations of the medicinal ingredients-Covid-19 exhibit that the relative energy has been impacted by the MC model of theory and various T(K), and the best consequences have been achieved for PE surface versus T(K) at the Monte Carlo methodology, and by enhancing T(K), our computations have remarked that as extrapolation features magnificently evaluate the medicinal ingredients-Covid-19 by the active site of a compound through nitrogen or oxygen critical points which are the sharpest part at the exhibited complex.

## Funding

This research received no external funding.

## Acknowledgments

The authors thank Professor Majid Monajjemi for their critical comments and evaluation.

## Conflicts of Interest

The authors declare no conflict of interest.

## References

1. White, D.B.; Lo, B. Mitigating Inequities and Saving Lives with ICU Triage during the COVID-19 Pandemic. *Am. J. Respir. Crit. Care Med.* **2021**, *203*, 287-295, <https://doi.org/10.1164/rccm.202010-3809CP>.
2. La Gatta, V.; Moscato, V.; Postiglione, M.; Sperli, G. An Epidemiological Neural Network Exploiting Dynamic Graph Structured Data Applied to the COVID-19 Outbreak. *IEEE Trans. Big Data* **2021**, *7*, 45-55, <https://doi.org/10.1109/TBDATA.2020.3032755>.
3. Vicidomini, C.; Roviello, V.; Roviello, G.N. In Silico Investigation on the Interaction of Chiral Phytochemicals from *Opuntia ficus-indica* with SARS-CoV-2 Mpro. *Symmetry* **2021**, *13*, 1041, <https://doi.org/10.3390/sym13061041>.
4. Theken, K.N.; Tang, S.Y.; Sengupta, S.; FitzGerald, G.A. The roles of lipids in SARS-CoV-2 viral replication and the host immune response. *J. Lipid Res.* **2021**, *62*, 100129, <https://doi.org/10.1016/j.jlr.2021.100129>.
5. Bhunjun, C.S.; Phillips, A.J.L.; Jayawardena, R.S.; Promputtha, I.; Hyde, K.D. Importance of Molecular Data to Identify Fungal Plant Pathogens and Guidelines for Pathogenicity Testing Based on Koch's Postulates. *Pathogens* **2021**, *10*, 1096, <https://doi.org/10.3390/pathogens10091096>.
6. Bharadwaj, S.; Dubey, A.; Yadava, U.; Mishra, S.K.; Kang, S.G.; Dwivedi, V.D. Exploration of natural compounds with anti-SARSCoV-2 activity via inhibition of SARS-CoV-2 Mpro. *Brief. Bioinform.* **2021**, *22*, 1361-1377, <https://doi.org/10.1093/bib/bbaa382>.
7. Rehman, T.; Al Ajmi, M.F.; Hussain, A. Natural compounds as inhibitors of SARS-CoV-2 main protease (3CLpro): A molecular docking and simulation approach to combat COVID-19. *Curr. Pharm. Des.* **2021**, *27*, 3577-3589, <https://doi.org/10.2174/1381612826999201116195851>.
8. Vicidomini, C.; Roviello, V.; Roviello, G.N. Molecular Basis of the Therapeutical Potential of Clove (*Syzygium aromaticum* L.) and Clues to Its Anti-COVID-19 Utility. *Molecules* **2021**, *26*, 1880, <https://doi.org/10.3390/molecules26071880>.
9. Mitton, B.; Rule, R.; Said, M. Laboratory evaluation of the BioFire FilmArray Pneumonia plus panel compared to conventional methods for the identification of bacteria in lower respiratory tract specimens: a prospective cross-sectional study from South Africa. *Diagn. Microbiol. Infect. Dis.* **2021**, *99*, 115236, <https://doi.org/10.1016/j.diagmicrobio.2020.115236>.
10. Waizel-Haiat, S.; Guerrero-Paz, J.A.; Sanchez-Hurtado, L.; Calleja-Alarcon, S.; Romero-Gutierrez, L. A case of fatal rhino-orbital mucormycosis associated with new Onset diabetic ketoacidosis and COVID-19. *Cureus* **2021**, *13*, e13163, <https://doi.org/10.7759/cureus.13163>.

11. Moraes, M.; Mendes, T.; Arantes, R. Smart Wearables for Cardiac Autonomic Monitoring in Isolated, Confined and Extreme Environments: A Perspective from Field Research in Antarctica. *Sensors* **2021**, *21*, 1303, <https://doi.org/10.3390/s21041303>.
12. Krupanidhi, S.; Abraham Peele, K.; Venkateswarulu, T.; Ayyagari, V.S.; Nazneen Bobby, M.; John Babu, D.; Venkata Narayana, A.; Aishwarya, G. Screening of phytochemical compounds of *Tinospora cordifolia* for their inhibitory activity on SARS-CoV-2: An in silico study. *J. Biomol. Struct. Dyn.* **2021**, *39*, 5799-5803, <https://doi.org/10.1080/07391102.2020.1787226>.
13. Hu, X.; Zhou, Z.; Li, F.; Xiao, Y.; Wang, Z.; Xu, J.; Dong, F.; Zheng, H.; Yu, R. The study of antiviral drugs targeting SARS-CoV-2 nucleocapsid and spike proteins through large-scale compound repurposing. *Heliyon* **2021**, *7*, e06387. <https://doi.org/10.1016/j.heliyon.2021.e06387>.
14. Mahmoud, A.; Mostafa, A.; Al-Karmalawy, A.A.; Zidan, A.; Abulkhair, H.S.; Mahmoud, S.H.; Shehata, M.; Elhefnawi, M.M.; Ali, M.A. Telaprevir is a potential drug for repurposing against SARS-CoV-2: Computational and in vitro studies. *Heliyon* **2021**, *7*, e07962, <https://doi.org/10.1016/j.heliyon.2021.e07962>.
15. Baildya, N.; Khan, A.A.; Ghosh, N.N.; Dutta, T.; Chattopadhyay, A.P. Screening of potential drug from *Azadirachta Indica* (Neem) extracts for SARS-CoV-2: An insight from molecular docking and MD-simulation studies. *J. Mol. Struct.* **2021**, *1227*, 129390, <https://doi.org/10.1016/j.molstruc.2020.129390>.
16. Aljahdali, M.O.; Molla, M.H.R.; Ahammad, F. Compounds identified from marine Mangrove plant (*Avicennia alba*) as potential antiviral drug candidates against WDSV, an in-silico approach. *Mar. Drugs* **2021**, *19*, 253, <https://doi.org/10.3390/md19050253>.
17. Revannavar, S.M.; Supriya, S.P.; Samaga, L.; Vineeth, V.K. COVID-19 triggering mucormycosis in a susceptible patient: A new phenomenon in the developing world? *BMJ Case Rep.* **2021**, *14*, e241663, <http://dx.doi.org/10.1136/bcr-2021-241663>.
18. Wadaa-Allah, A.; Emhamed, M.S.; Sadeq, M.A.; Dahman, N.B.H.; Ullah, I.; Farrag, N.S.; Negida, A. Efficacy of the current investigational drugs for the treatment of COVID-19: A scoping review. *Ann. Med.* **2021**, *53*, 318-334, <https://doi.org/10.1080/07853890.2021.1875500>.
19. Luo, H.; Yang, M.; Tang, Q.L.; Hu, X.Y.; Willcox, M.L.; Liu, J.P. Characteristics of registered clinical trials on traditional Chinese medicine for coronavirus disease 2019 (COVID-19): A scoping review. *Eur. J. Integr. Med.* **2021**, *41*, 101251, <https://doi.org/10.1016/j.eujim.2020.101251>.
20. Bajgain, K.T.; Badal, S.; Bajgain, B.B.; Santana, M.J. Prevalence of comorbidities among individuals with COVID-19: A rapid review of current literature. *Am. J. Infect. Control* **2021**, *49*, 238-246, <https://doi.org/10.1016/j.ajic.2020.06.213>.
21. Bakhshi, K.; Mollaamin, F.; Monajjemi, M. Exchange and Correlation Effect of Hydrogen Chemisorption on Nano V(100) Surface: A DFT Study by Generalized Gradient Approximation (GGA). *Journal of Computational and Theoretical Nanoscience* **2011**, *8*, 763-768, <https://doi.org/10.1166/jctn.2011.1750>.
22. Haidere, M.F.; Ratan, Z.A.; Nowroz, S.; Bin Zaman, S.; Jung, Y.-J.; Hosseinzadeh, H.; Cho, J.Y. COVID-19 Vaccine: Critical questions with complicated answers. *Biomol. Ther.* **2021**, *29*, 1-10, <https://doi.org/10.4062/biomolther.2020.178>.
23. Kunz Coyne, A.J.; Casapao, A.M.; Isache, C.; Morales, J.; McCarter, Y.S.; Jankowski, C.A. Influence of Antimicrobial Stewardship and Molecular Rapid Diagnostic Tests on Antimicrobial Prescribing for Extended-Spectrum Beta-Lactamase- and Carbapenemase-Producing *Escherichia coli* and *Klebsiella pneumoniae* in Bloodstream Infection. *Microbiol. Spectr.* **2021**, *9*, e0046421, <https://doi.org/10.1128/Spectrum.00464-21>.
24. Zamri, A.S.; Singh, S.; Ghazali, S.M.; Heng, L.C.; Dass, S.C.; Aris, T.; Ibrahim, H.M.; Gill, B.S. Effectiveness of the movement control measures during the third wave of COVID-19 in Malaysia. *Epidemiol. Health* **2021**, *43*, e2021073, <https://doi.org/10.4178/epih.e2021073>.
25. Xiong, P.; Zhang, H.; Li, G.; Liao, C.; Jiang, G. Adsorption removal of ibuprofen and naproxen from aqueous solution with Cu-doped MIL-101(Fe). *Sci. Total. Environ.* **2021**, *797*, 149179, <https://doi.org/10.1016/j.scitotenv.2021.149179>.
26. Oran, D.P.; Topol, E.J. The Proportion of SARS-CoV-2 Infections That Are Asymptomatic: A Systematic Review. *Ann. Intern. Med.* **2021**, *174*, 655-662, <https://doi.org/10.7326/M20-6976>.
27. Tan, R.Q.; Li, W.T.V.; Shum, W.Z.; Chu, S.C.; Li, H.L.; Shea, Y.F.; Chung, T.W. A systematic review and meta-analysis protocol examining the clinical characteristics and epidemiological features of olfactory dysfunction (OD) in coronavirus disease 2019 (COVID-19). *Syst. Rev.* **2021**, *10*, 73, <https://doi.org/10.1186/s13643-021-01624-6>.

28. Zadeh, M.A.A.; Lari, H.; Kharghanian, L.; Balali, E.; Khadivi, R.; Yahyaei, H.; Mollaamin, F.; Monajjemi, M. Density Functional Theory Study and Anti-Cancer Properties of Shyshaq Plant: In View Point of Nano Biotechnology. *J Comput Theor Nanosci* **2015**, *12*, 4358-4367, <https://doi.org/10.1166/jctn.2015.4366>.
29. Badshah, S.L.; Faisal, S.; Muhammad, A.; Poulson, B.G.; Emwas, A.H.; Jaremko, M. Antiviral activities of flavonoids. *Biomed. Pharmacother.* **2021**, *140*, 111596, <https://doi.org/10.1016/j.biopha.2021.111596>.
30. Eberle, R.J.; Olivier, D.S.; Pacca, C.C.; Avilla, C.M.S.; Nogueira, M.L.; Amaral, M.S.; Willbold, D.; Arni, R.K.; Coronado, M.A. In vitro study of Hesperetin and Hesperidin as inhibitors of zika and chikungunya virus proteases. *PLoS ONE* **2021**, *16*, e0246319, <https://doi.org/10.1371/journal.pone.0246319>.
31. Mallah, S.I.; Ghorab, O.K.; Al-Salmi, S.; Abdellatif, O.S.; Tharmaratnam, T.; Iskandar, M.A.; Sefen, J.A.N.; Sidhu, P.; Atallah, B.; El-Lababidi, R.; Al-Qahtabi, M. COVID-19: Breaking down a global health crisis. *Ann. Clin. Microbiol. Antimicrob.* **2021**, *20*, 1-36, <https://doi.org/10.1186/s12941-021-00438-7>.
32. Akbulut, S. Medicinal Plants Preferences for the Treatment of COVID-19 Symptoms in Central and Eastern Anatolia. *Kastamonu Univ. Journal of Forestry Faculty* **2021**, *21*, 196-207, <https://doi.org/10.17475/kastorman.1048372>.
33. Frisch, M.J.; Trucks, G.W.; Schlegel, H.B.; Scuseria, G.E.; Robb, M.A.; Cheeseman, J.R.; Scalmani, G.; et al. *Gaussian 09, Revision B.01*. **2010**. Gaussian Inc., Wallingford.
34. Mollaamin, F.; Monajjemi, M. Harmonic Linear Combination and Normal Mode Analysis of Semiconductor Nanotubes Vibrations. *J. Comput. Theor. Nanosci.* **2015**, *12*, 1030-1039, <https://doi.org/10.1166/jctn.2015.3846>.
35. Monajjemi, M.; Khaleghian, M.; Tadayonpour, N.; Mollaamin, F. The effect of different solvents and temperatures on stability of single-walled carbon nanotube: a QM/MD study. *Int. J. Nanosci.* **2010**, *9*, 517, <https://doi.org/10.1142/S0219581X10007071>.
36. Tahan, A.; Mollaamin, F.; Monajjemi, M. Thermochemistry and NBO analysis of peptide bond: Investigation of basis sets and binding energy. *Russian Journal of Physical Chemistry A* **2009**, *83*, 587-597, <https://doi.org/10.1134/S003602440904013X>.
37. Monajjemi, M.; Afsharnezhad, S.; Jaafari, M.R.; Mirdamadi, S.; Mollaamin, F.; Monajjemi, H. Investigation of energy and NMR isotropic shift on the internal rotation Barrier of  $\Theta_4$  dihedral angle of the DLPC: A GIAO study. *Chemistry* **2008**, *17*, 55-69.
38. Monajjemi, M.; Honarparvar, B.; Khalili Hadad, B.; Ilkhani, A.; Mollaamin, F. Thermo-Chemical Investigation and NBO Analysis of Some anxiolytic as Nano- Drugs. *African journal of pharmacy and pharmacology* **2010**, *4*, 521-529.
39. Monajjemi, M.; Mahdavian, L.; Mollaamin, F.; Khaleghian, M. Interaction of Na, Mg, Al, Si with carbon nanotube (CNT): NMR and IR study. *Russ. J. Inorg. Chem* **2009**, *54*, 1465-1473, <https://doi.org/10.1134/S0036023609090216>.
40. Monajjemi, M.; Lee, V.S.; Khaleghian, M.; Honarparvar, B.; Mollaamin, F. Theoretical Description of Electromagnetic Nonbonded Interactions of Radical, Cationic, and Anionic NH<sub>2</sub>BHNBH<sub>2</sub> Inside of the B18N18 Nanoring. *J. Phys. Chem C* **2010**, *114*, 15315-15330, <https://doi.org/10.1021/jp104274z>.
41. Gómez, S.; Egidi, F.; Puglisi, A.; Giovannini, T.; Rossi, B.; Cappelli, C. Unlocking the Power of Resonance Raman Spectroscopy: The Case of Amides in Aqueous Solution. *J. Mol. Liq.* **2021**, *346*, 117841, <https://doi.org/10.1016/j.molliq.2021.117841>.
42. Monajjemi, M.; Mollaamin, F.; Gholami, M.R.; Yoosbashizadeh, H.; Sadrnezhad, S.K.; Passdar, H. Quantum chemical parameters of some organic corrosion inhibitors, pyridine, 2-picoline 4-picoline and 2,4-lutidine, adsorption at aluminum surface in hydrochloric and nitric acids and comparison between two acidic media. *Main Group Met. Chem.* **2003**, *26*, 349-361, <https://doi.org/10.1515/MGMC.2003.26.6.349>.
43. Ni, W.; Li, G.; Zhao, J.; Cui, J.; Wang, R.; Gao, Z.; Liu, Y. Use of Monte Carlo simulation to evaluate the efficacy of tigecycline and minocycline for the treatment of pneumonia due to carbapenemase-producing *Klebsiella pneumoniae*. *Infect Dis* **2018**, *50*, 507-513, <http://doi.org/10.1080/23744235.2018.1423703>.
44. Andrews, C.W.; Wisowaty, J.; Davis, A.O.; Crouch, R.C.; Martin, G.E. Molecular modeling, NMR spectroscopy, and conformational analysis of 3',4'-anhydrovinblastine. *J. Heterocycl. Chem.* **1995**, *32*, 1011-1017, <https://doi.org/10.1002/jhet.5570320357>.
45. HyperChem, version 8.0; Hypercube Inc: Gainesville, FL, USA (**2007**).
46. Sarasia, E.M.; Afsharnezhad, S.; Honarparvar, B.; Mollaamin, F.; Monajjemi, M. Theoretical study of solvent effect on NMR shielding tensors of luciferin derivatives. *Phys. Chem. Liq.* **2011**, *49*, 561-571, <https://doi.org/10.1080/00319101003698992>.



47. Monajjemi, M.; Noei, M.; Mollaamin, F. Design of fMet-tRNA and calculation of its bonding properties by quantum mechanics. *Nucleosides, Nucleotides and Nucleic Acids* **2010**, *29*, 9, <https://doi.org/10.1080/15257771003781642>.
48. Ghalandari, B.; Monajjemi, M.; Mollaamin, F. Theoretical Investigation of Carbon Nanotube Binding to DNA in View of Drug Delivery. *J.Comput.Theor.Nanosci* **2011**, *8*, 1212-1219, <https://doi.org/10.1166/jctn.2011.1801>.
49. Monajjemi, M.; Farahani, N.; Mollaamin, F. Thermodynamic study of solvent effects on nanostructures: Phosphatidylserine and phosphatidylinositol membranes. *Phys. Chem. Liq* **2012**, *50*, 161-172, <https://doi.org/10.1080/00319104.2010.527842>.
50. Khaleghian, M.; Zahmatkesh, M.; Mollaamin, F.; Monajjemi, M. Investigation of Solvent Effects on Armchair Single-Walled Carbon Nanotubes: A QM/MD Study. *Fuller. Nanotub. Carbon Nanostructures* **2011**, *19*, 251-261, <https://doi.org/10.1080/15363831003721757>.
51. Mollaamin, F.; Monajjemi, M.; Salemi, S.; Baei, M.T. A Dielectric Effect on Normal Mode Analysis and Symmetry of BNNT Nanotube. *Fuller. Nanotub. Carbon Nanostructures* **2011**, *19*, 182-196, <https://doi.org/10.1080/15363831003782932>.
52. Monajjemi, M.; Baie, M.T.; Mollaamin, F. Interaction between threonine and cadmium cation in [Cd(Thr)<sub>n</sub>]<sup>2+</sup> (n = 1–3) complexes: density functional calculations. *Russian Chemical Bulletin* **2010**, *59*, 886-889, <https://doi.org/10.1007/s11172-010-0181-5>.
53. Feldman, C.; Anderson, R. The role of co-infections and secondary infections in patients with COVID-19. *Pneumonia (Nathan)* **2021**, *13*, 5. <https://doi.org/10.1186/s41479-021-00083-w>.
54. Ye, S.; Zhang, Y.; Zhao, X.; Yu, Z.; Song, Y.; Tan, Z.; Tang, Y.; Chen, S.; Wang, M.; Ling, H. Emerging Variants of B.1.617 Lineage Identified Among Returning Chinese Employees Working in India-Chongqing Municipality, China, April 2021. *China CDC Wkly.* **2021**, *3*, 409–410. <https://doi.org/10.46234/ccdcw2021.109>.
55. Jacob, J.J.; Fletcher, J.G.; Priya, M.T.; Veeraraghavan, B.; Mutreja, A. Relevance of immune response and vaccination strategies of SARS-CoV-2 in the phase of viral red queen dynamics. *Indian J. Med. Microbiol.* **2021**, *39*, 417–422. <http://doi.org/10.1016/j.ijmmb.2021.08.001>.
56. Singh, J.; Rahman, S.A.; Ehtesham, N.Z.; Hira, S.; Hasnain, S.E. SARS-CoV-2 variants of concern are emerging in India. *Nat. Med.* **2021**, *27*, 1131–1133. <https://doi.org/10.1038/s41591-021-01397-4>.
57. Mlcochova, P.; Kemp, S.; Dhar, M.S.; Papa, G.; Meng, B.; Ferreira, I.A.T.M.; Datir, R.; Collier, D.A.; Albecka, A.; Singh, S.; et al. Indian SARS-CoV-2 Genomics Consortium (INSACOG); Genotype to Phenotype Japan (G2P-Japan) Consortium; CITIID-NIHR BioResource COVID-19 Collaboration. SARS-CoV-2 B.1.617.2 Delta variant replication and immune evasion. *Nature* **2021**, *599*, 114–119. <https://doi.org/10.1038/s41586-021-03944-y>.
58. Plante, J.A.; Liu, Y.; Liu, J.; Xia, H.; Johnson, B.A.; Lokugamage, K.G.; Zhang, X.; Muruato, A.E.; Zou, J.; Fontes-Garfias, C.R.; et al. Spike mutation D614G alters SARS-CoV-2 fitness. *Nature* **2021**, *592*, 116–121. <https://doi.org/10.1038/s41586-020-2895-3>.
59. Chung, J.Y.; Thone, M.N.; Kwon, Y.J. COVID-19 vaccines: The status and perspectives in delivery points of view. *Adv. Drug Deliv. Rev.* **2021**, *170*, 1–25. <https://doi.org/10.1016/j.addr.2020.12.011>.
60. Joshi, C.; Chaudhari, A.; Joshi, C.; Joshi, M.; Bagatharia, S. Repurposing of the herbal formulations: Molecular docking and molecular dynamics simulation studies to validate the efficacy of phytochemicals against SARS-CoV-2 proteins. *J. Biomol. Struct. Dyn.* **2021**, *14*, 1–15. <https://doi.org/10.1080/07391102.2021.1922095>.
61. Vicidomini, C.; Roviello, V.; Roviello, G.N. Molecular Basis of the Therapeutical Potential of Clove (*Syzygium aromaticum* L.) and Clues to Its Anti-COVID-19 Utility. *Molecules* **2021**, *26*, 1880. <https://doi.org/10.3390/molecules26071880>.
62. Das, A.; Pandita, D.; Jain, G.K.; Agarwal, P.; Grewal, A.S.; Khar, R.K.; Lather, V. Role of phytoconstituents in the management of COVID-19. *Chem. Biol. Interact.* **2021**, *341*, 109449. <https://doi.org/10.1016/j.cbi.2021.109449>.
63. Monajjemi, M.; Jafari Azan, M.; Mollaamin, F. Density functional theory study on B30N20 nanocage in structural properties and thermochemical outlook. *Fullerenes Nanotubes and Carbon Nanostructures* **2013**, *21*, 503-515, <https://doi.org/10.1080/1536383X.2011.629762>.
64. Monajjemi, M.; Bagheri, S.; Moosavi, M.S. et al. Symmetry breaking of B2N(-,0,+): An aspect of the electric potential and atomic charges. *Molecules* **2015**, *20*, 21636-21657, <https://doi.org/10.3390/molecules201219769>.

65. Mahdavian, L.; Monajjemi, M. Alcohol sensors based on SWNT as chemical sensors: Monte Carlo and Langevin dynamics simulation. *Microelectronics journal* **2010**, *41*, 142-149, <https://doi.org/10.1016/j.mejo.2010.01.011>.
66. Monajjemi, M. Cell membrane causes the lipid bilayers to behave as variable capacitors: A resonance with self-induction of helical proteins. *Biophysical Chemistry* **2015**, *207*, 114-127, <https://doi.org/10.1016/j.bpc.2015.10.003>.
67. Monajjemi, M. Liquid-phase exfoliation (LPE) of graphite towards graphene: An ab initio study. *Journal of Molecular Liquids* **2017**, *230*, 461-472, <https://doi.org/10.1016/j.molliq.2017.01.044>.
68. Monajjemi, M.; Mohammadian, N.T. S-NICS: An aromaticity criterion for nano molecules. *Journal of Computational and Theoretical Nanoscience* **2015**, *12*, 4895-4914, <https://doi.org/10.1166/jctn.2015.4458>.
69. Monajjemi, M.; Boggs, J.E. A New Generation of BnNn Rings as a Supplement to Boron Nitride Tubes and Cages. *J. Phys. Chem. A* **2013**, *117*, 1670-1684, <http://dx.doi.org/10.1021/jp312073q>.
70. Monajjemi, M. Non bonded interaction between BnNn (stator) and BN B (rotor) systems: A quantum rotation in IR region. *Chemical Physics* **2013**, *425*, 29-45, <https://doi.org/10.1016/j.chemphys.2013.07.014>.
71. Monajjemi, M.; Robert, W.J.; Boggs, J.E. NMR contour maps as a new parameter of carboxyl's OH groups in amino acids recognition: A reason of tRNA-amino acid conjugation. *Chemical Physics* **2014**, *433*, 1-11, <https://doi.org/10.1016/j.chemphys.2014.01.017>.
72. Monajjemi, M. Quantum investigation of non-bonded interaction between the B15N15 ring and BH2NBH2 (radical, cation, and anion) systems: a nano molecular motor. *Struct Chem* **2012**, *23*, 551-580, <http://dx.doi.org/10.1007/s11224-011-9895-8>.
73. Monajjemi, M. Metal-doped graphene layers composed with boron nitride-graphene as an insulator: a nanocapacitor. *Journal of Molecular Modeling* **2014**, *20*, 2507, <https://doi.org/10.1007/s00894-014-2507-y>.
74. Monajjemi, M.; Heshmat, M.; Haeri, H.H.; Kaveh, F. Theoretical study of vitamin properties from combined QM-MM methods: Comparison of chemical shifts and energy. *Russian Journal of Physical Chemistry* **2006**, *80*, 1061, <https://doi.org/10.1134/S0036024406070119>.
75. Christy, M.; Uekusa, Y.; Gerwick, L.; Gerwick, W. Natural Products with Potential to Treat RNA Virus Pathogens Including SARS-CoV-2. *J. Nat. Prod.* **2021**, *84*, 161-182, <https://doi.org/10.1021/acs.jnatprod.0c00968>.
76. Monajjemi, M.; Najafpour, J.; Mollaamin, F. (3,3)<sub>4</sub> Armchair carbon nanotube in connection with PNP and NPN junctions: Ab Initio and DFT-based studies. *Fullerenes Nanotubes and Carbon Nanostructures* **2013**, *21*, 213-232, <https://doi.org/10.1080/1536383X.2011.597010>.
77. Monajjemi, M.; Baheri, H.; Mollaamin, F. A percolation model for carbon nanotube-polymer composites using the Mandelbrot-Given. *Journal of Structural Chemistry* **2011**, *52*, 54-59, <https://doi.org/10.1134/S0022476611010070>.
78. Antonescu, A.-I.; Miere, F.; Fritea, L.; Ganea, M.; Zdrinca, M.; Dobjanschi, L.; Antonescu, A.; Vicas, S.I.; Bodog, F.; Sindhu, R.K.; et al. Perspectives on the Combined Effects of Ocimum basilicum and Trifolium pratense Extracts in Terms of Phytochemical Profile and Pharmacological Effects. *Plants* **2021**, *10*, 1390. <https://doi.org/10.3390/plants10071390>.
79. Kulyar, M.F.; Li, R.; Mehmood, K.; Waqas, M.; Li, K.; Li, J. Potential influence of Nagella sativa (Black cumin) in reinforcing immune system: A hope to decelerate the COVID-19 pandemic. *Phytomedicine* **2021**, *85*, 153277. <https://doi.org/10.1016/j.phymed.2020.153277>.
80. Zhao, X.; Chen, H.; Wang, H. Glycans of SARS-CoV-2 Spike Protein in Virus Infection and Antibody Production. *Front. Mol. Biosci.* **2021**, *8*, 629873. <https://doi.org/10.3389/fmolb.2021.629873>.
81. Baral, P.; Bhattarai, N.; Hossen, M.L.; Stebliankin, V.; Gerstman, B.S.; Narasimhan, G.; Chapagain, P.P. Mutation-induced changes in the receptor-binding interface of the SARS-CoV-2 Delta variant B.1.617.2 and implications for immune evasion. *Biochem. Biophys. Res. Commun.* **2021**, *574*, 14-19. <https://doi.org/10.1016/j.bbrc.2021.08.036>.
82. Banerjee, A.; Kanwar, M.; Mohapatra, P.K.D.; Saso, L.; Nicoletti, M.; Maiti, S. Nigellidine (Nigella sativa, black-cumin seed) docking to SARS CoV-2 nsp3 and host inflammatory proteins may inhibit viral replication/transcription and FAS-TNF death signal via TNFR 1/2 blocking. *Nat. Prod. Res.* **2021**, 1-6. <https://doi.org/10.1080/14786419.2021.2018430>.